Title

The hepatic compensatory response to elevated systemic sulfide impairs medium chain fat oxidation and promotes diabetes.

Authors

Roderick N. Carter[1], Matthew T.G. Gibbins[1,2], Martin E. Barrios-Llerena[1,3], Stephen Wilkie[1,3], Peter Freddolino[4], Marouane Libiad[5,6], Victor Vitvitsky[5], Barry Emerson[1,7], Thierry LeBihan[8,9], Madara Brice[1], Huizhong Su[10,11], Scott Denham[1], Natalie Z.M. Homer[1], Clare Mc Fadden[1,12], Anne Tailleux[13], Nourdine Faresse[14,15], Thierry Sulpice[14], Francois Briand[14], Tom Gillingwater[16], Kyo Han Ahn[17], Subhankar Singha[17,18], Claire McMaster[19], Richard C. Hartley[19], Bart Staels[13], Gillian Gray[1], Andrew J. Finch[10,20], Colin Selman[4], Ruma Banerjee[5], Nicholas M. Morton[1*]

[1]University/British Heart Foundation Centre for Cardiovascular Science, University of Edinburgh, Queen's Medical Research Institute, Edinburgh, EH16 4TJ, United Kingdom
[2]Royal Papsworth Hospital NHS Foundation Trust, Cambridge, CB2 0AY, United Kingdom
[3]St. Anne's University Hospital, Brno, 656 91, Czech Republic
[4]Glasgow Ageing Research Network (GARNER), Institute of Biodiversity, Animal Health and Comparative Medicine, University of Glasgow, Glasgow, G12 8QQ, United Kingdom
[5]The Department of Biological Chemistry, University of Michigan Medical School, Ann Arbor, MI 48109, USA
[6]Institute for Integrative Biology of the Cell (I2BC), CEA, CNRS, Univ. Paris-Sud, Université Paris-Saclay, 91198, Gif-sur-Yvette cedex, France
[7]BD Research Centre Ireland, Co. Limerick, Castletroy, Ireland
[8]SynthSys - Systems and Synthethic Biology, Edinburgh, EH9 3JD, United Kingdom
[9]Rapid Novor Inc, 44 Gaukel St, Kitchener, ON N2G 4P3, Canada
[10]Cancer Research UK Edinburgh Centre, MRC Intitute of Genetics & Molecular Medicine, University of Edinburgh, Western General Hospital, Edinburgh, EH4 2XR, United Kingdom
[11]Wellcome Trust Centre for Mitochondrial Research, Newcastle University, NE2 4HH, United Kingdom
[12]Springer Nature Campus, London, N1 9FN, United Kingdom
[13]Université de Lille, Inserm, CHU Lille, Institut Pasteur de Lille, U101-EGID, F-59000, Lille, France
[14]Physiogenex S.A.S, Prologue Biotech, 516 rue Pierre et Marie Curie, 31670 Labège, France
[15]D.I.V.A-expertise, 1 place Pierre Potier, 31100 Toulouse, France
[16]College of Medicine & Veterinary Medicine, University of Edinburgh, Old Medical School (Anatomy), Teviot Place, Edinburgh, EH8 9AG, United Kingdom
[17]Department of Chemistry, POSTECH, 77 Cheongam-Ro, Nam-Gu, Pohang, Gyungbuk, 37673, South Korea
[18]Institute of Advanced Studies and Research, JIS University, Kolkata 700091, India
[19]School of Chemistry, Joseph Black Building, University of Glasgow, Glasgow, G12 8QQ, United Kingdom
[20]Cancer Research UK Barts Centre, London, EC1M 6BQ, United Kingdom

[*]Lead Contact details: Nicholas M Morton
Molecular Metabolism Group, University/British Heart Foundation Centre for Cardiovascular Science, University of Edinburgh, Queen's Medical Research Institute, Edinburgh, EH16 4TJ, United Kingdom.
nik.morton@ed.ac.uk

Competing interests statement,

The authors have declared that no conflict of interest exists.

Abstract

Impaired hepatic glucose and lipid metabolism are hallmarks of type–2 diabetes. Increased sulfide production from cysteine, or sulfide–donor compounds, may beneficially regulate hepatic metabolism. Disposal of sulfide through the sulfide oxidation pathway (SOP) is critical for maintaining sulfide within a safe physiological range. We show that mice lacking the liver–enriched mitochondrial SOP enzyme thiosulfate sulfur–transferase (*Tst*$^{-/-}$ mice) exhibit high circulating sulfide, increased gluconeogenesis, hypertriglyceridemia and fatty liver, despite whole–body insulin–sensitisation. Unexpectedly, hepatic sulfide levels were normal in *Tst*$^{-/-}$ mice, a result of homeostatic induction of mitochondrial sulfide disposal and glutathione excretion associated with net suppression of protein persulfidation and nuclear respiratory factor–2 target proteins. Proteomic and persulfidomic profiling converged on hepatic lipid metabolism, revealing a deficit in medium–chain fatty acid oxidation in *Tst*$^{-/-}$ mice. In conclusion our findings have implications for sulfide-donor strategies in the context of liver function and metabolic disease.

62 # Introduction

63 The prevalence of Type 2 diabetes (T2D) continues to soar in parallel with that of obesity[1].
64 Increased hepatic glucose production and aberrant hepatic lipid metabolism are cardinal
65 features of T2D[2,3]. Dysregulation of hepatic nutrient metabolism in T2D is a promising area
66 for therapeutic intervention because it precipitates the more severe liver pathologies that
67 manifest along the spectrum of non-alcoholic fatty liver disease (NAFLD), steatosis,
68 steatohepatitis and hepatocellular carcinoma[4].

69 Hydrogen sulfide (hereafter referred to as sulfide), an endogenously produced gaseous
70 signalling molecule[5–8], has recently emerged as a modulator of nutrient metabolism[9–12].
71 Enzymatic sulfide production from sulfur amino acids is catalysed by cystathionine beta–
72 synthase; CBS, and cystathionine gamma lyase; CTH[13,14] and by 3-mercaptopyruvate sulfur
73 transferase; MPST[15–17]. Thioredoxin-mediated reduction of cysteine persulfides on proteins
74 also regulates free sulfide and cysteine persulfide levels[18]. Endogenously produced and
75 exogenously administered sulfide specifically influences hepatic glucose and lipid
76 metabolism[19,20]. Thus, *in vitro,* treatment of murine hepatocytes with NaHS, or
77 overexpression of rat *Cth* in HepG2 liver cells, increased glucose production through increased
78 gluconeogenesis and reduced glycogen storage[21]. Conversely, glucose production was lower
79 in hepatocytes from *Cth* gene knockout mice (*Cth*$^{-/-}$ mice) that exhibit low sulfide
80 production[21]. Elevation of sulfide with NaHS administration *in vivo* reduced cholesterol and
81 triglyceride accumulation in the liver of high fat diet (HFD)–fed mice[22]. In contrast, inter-cross
82 of sulfide production–deficient *Cth*$^{-/-}$ mice with the hyperlipidemic *Apoe*$^{-/-}$ mouse strain
83 (*Cth*$^{-/-}$*Apoe*$^{-/-}$ mice) produced a phenotype of elevated plasma cholesterol following
84 exposure to an atherogenic diet[23]. Consistent with their higher cholesterol, *Cth*$^{-/-}$*Apoe*$^{-/-}$
85 mice developed fatty streak lesions earlier than *Apoe*$^{-/-}$ mice, and this effect was reversed

86 by NaHS administration[23]. Sulfide may also indirectly impact hepatic nutrient metabolism
87 through its effect on hepatic artery vasorelaxation and thus liver perfusion[24,25]. The
88 apparently beneficial effects of sulfide administration in multiple disease indications has led
89 to a major drive towards development of targeted H_2S–donor molecules as a therapeutic
90 approach[26,27]. However, an often-overlooked aspect of net sulfide exposure, key to the
91 efficacy of therapeutic H_2S–donors, is that it is regulated through its oxidative disposal. Thus,
92 endogenous sulfide exposure is actively limited to prevent mitochondrial respiratory
93 toxicity[28–30]. Sulfide is rapidly oxidized[31,32] through the mitochondrial sulfide oxidation
94 pathway (SOP), consisting of sulfide quinone oxidoreductase (SQOR), persulfide dioxygenase
95 (ETHE1/PDO) and thiosulfate sulfurtransferase (TST, also known as rhodanese)[31,33,34]. The
96 liver is highly abundant in SOP enzymes, and is a major organ of whole body sulfide disposal[32].
97 Mice lacking the *Ethe1* gene (*Ethe1*$^{-/-}$ mice) die of fatal sulfide toxicity[30], consistent with its
98 critical role in sulfide oxidation and the severe pathological consequences of unchecked
99 sulfide build-up in tissues. However, the importance of mitochondrial TST in the SOP *in vivo*
100 remains obscure. In contrast to *Ethe1*$^{-/-}$ mice, *Tst*$^{-/-}$ mice were grossly normal despite
101 exhibiting substantially elevated blood sulfide levels, as implied by qualitative measures[35].
102 This revealed an important yet distinct role for TST in the SOP for the first time *in vivo*.
103 Nevertheless, *Tst*$^{-/-}$ mice showed an apparently diabetogenic impairment of glucose
104 tolerance[35], consistent with the concept that increased sulfide promotes hepatic glucose
105 production[21]. As *Tst* deficiency represents a model of chronic but viable sulfide elevation,
106 determining the molecular mechanisms driving their aberrant metabolic profile can provide
107 important insights into the optimal range for therapeutic sulfide exposure, particularly in light
108 of the current interest in developing mitochondrially–targeted sulfide–donors[36,37]. To this end

109 we sought to define the impact of *Tst* deficiency on the underlying molecular pathways that

110 impact hepatic metabolism.

111

112 # Results

113 *Tst*$^{-/-}$ *mice exhibit increased hepatic gluconeogenesis and dyslipidaemia despite peripheral*
114 *insulin sensitisation.* TST *mRNA* expression is highest in the liver (e.g. it is ~8-fold higher than
115 in white adipose tissue http://biogps.org/#goto=genereport&id=22117). We therefore
116 hypothesised that liver TST deficiency was the principal driver of the impaired glucose
117 tolerance observed in *Tst*$^{-/-}$ mice[35]. We first tested this by challenging the mice with
118 pyruvate, which is converted to glucose in the liver. *Tst*$^{-/-}$ mice exhibited higher glucose
119 production than C57BL/6J controls in response to pyruvate (Figure 1A). We next tested
120 phosphoenolpyruvate carboxykinase (PEPCK) activity, the rate-determining enzyme in *de-*
121 *novo* hepatic glucose synthesis, and found it was higher in liver homogenates from *Tst*$^{-/-}$
122 mice (Figure 1B). Next, we traced the metabolite incorporation of $^{13}C_3$-pyruvate by isolated
123 *Tst*$^{-/-}$ hepatocytes, which showed a significant reduction in $^{13}C_2$-acetyl-CoA and a significant
124 increase in $^{13}C_3$-aspartate, consistent with skewing of the tricarboxylic acid cycle towards
125 gluconeogenic precursors (Figure 1C). We also assessed whether *Tst* deficiency is associated
126 with impaired lipid metabolism, another hallmark of diabetes. Fast protein liquid
127 chromatography analysis of triglyceride levels and their lipoprotein distribution revealed
128 significantly higher total plasma triglycerides in *Tst*$^{-/-}$ mice (Figure 1D). The higher
129 triglyceride was selectively associated with an increased VLDL triglyceride fraction (Figure 1D),
130 consistent with a dominant liver-driven impairment in lipid metabolism[38]. Total and distinct
131 lipoprotein fraction plasma cholesterol levels were similar between genotypes (Figure S1A
132 and S1B), suggestive of a triglyceride–selective effect of *Tst* deficiency on hepatic lipid efflux.
133 HFD significantly increased liver lipid content of C57BL/6J mice but did not further increase
134 the lipid levels in the liver of *Tst*$^{-/-}$ mice (Figure 1E-1F). Liver glycogen, a marker of long–term

135 carbohydrate storage was comparable between *Tst*$^{-/-}$ and C57BL/6J control mice (Figure
136 S1C). Steady–state phosphorylation levels of hepatic insulin–responsive proteins AKT and the
137 cellular energy–sensing protein AMPK were comparable between *Tst*$^{-/-}$ mice and C57BL/6J
138 littermates (Figure S1D).

139 Despite unchanged steady–state markers of hepatic insulin sensitivity, impaired glucose
140 tolerance suggested that whole body, and usually hepatic, insulin–resistance was present. To
141 test this, we performed an insulin tolerance test. Unexpectedly, the glucose decrement in
142 response to insulin was greater in *Tst*$^{-/-}$ mice (Figure 1G), demonstrating a net increase in
143 dynamic whole–body insulin sensitivity despite increased hepatic glucose output. We
144 confirmed increased whole–body insulin sensitivity under short–term steady–state
145 conditions using euglycaemic hyperinsulinaemic clamps. Blood glucose tended to be higher
146 in the *Tst*$^{-/-}$ mice during baseline conditions (Figure 1H). During the clamp, when blood
147 glucose levels were maintained constant, the glucose infusion rate was comparable between
148 genotypes (Table S1). However, an overall increase in glucose uptake (integral glucose) by
149 tissues in the *Tst*$^{-/-}$ mice was apparent (Figure 1I, Table S1), supporting increased peripheral
150 insulin–sensitivity concurrent with higher endogenous glucose production. After HFD feeding,
151 *Tst*$^{-/-}$ mice exhibited relatively lower fasting insulin and higher hepatic glucose output across
152 baseline pre-clamp conditions (Table S2). However, the metabolic phenotype of *Tst*$^{-/-}$ mice
153 largely converged on that of the C57BL/6J mice during the hyperinsulinemic clamp (Table S2).

154 *TST deficiency elicits compensatory hepatic sulfide disposal mechanisms that drive reduced*
155 *global protein persulfidation.* A role for TST in the disposal of sulfide was suggested by its
156 participation in the SOP[31,34] and supported *in vivo* by the qualitatively higher blood sulfide of
157 *Tst*$^{-/-}$ mice[35]. Here, we quantified circulating sulfide, showing approximately 10–fold
158 elevation in the blood and plasma of *Tst*$^{-/-}$ mice (Table 1A and 1B). Thiosulfate, an oxidised

159 metabolite of sulfide [39,40] and a TST substrate[41], was approximately 20–fold higher in plasma
160 (Table 1B), and profoundly higher (450–fold) in urine (Table 1C) of *Tst*$^{-/-}$ mice compared to
161 C57Bl/6J mice. Reduced glutathione (GSH) levels were ~2–fold higher in the plasma of *Tst*$^{-/-}$
162 mice (Table 1B). To determine any direct hepatic contribution to the elevated systemic sulfide
163 *in vivo*, whole blood was sampled from the inferior vena cava (IVC) (Table 1D). IVC sulfide
164 levels tended to be higher in the *Tst*$^{-/-}$ mice, but the magnitude of the increase (~3-fold) did
165 not parallel that in trunk blood (~10-fold), suggesting liver was not a major source of the
166 elevated circulating sulfide. Surprisingly, liver sulfide, thiosulfate, cysteine and GSH levels
167 were similar between *Tst*$^{-/-}$ and C57BL/6J mice (Table 1E). Further, cultured hepatocytes
168 from *Tst*$^{-/-}$ and C57BL/6J mice exhibited similar intracellular sulfide levels, as estimated
169 using P3, a sulfide–selective fluorescent probe[42] (Table 1F). Mitochondrial sulfide levels in
170 liver reported by MitoA/MitoN[43] were similarly unchanged between genotypes (Table 1G).
171 The apparently unaltered hepatic steady-state sulfide levels, despite higher circulating
172 sulfide, suggested a profound homeostatic mechanism was invoked in the liver of *Tst*$^{-/-}$
173 mice. We assessed respiratory sulfide disposal (antimycin–sensitive) and found this was
174 markedly increased in hepatocytes from *Tst*$^{-/-}$ mice, whereas antimycin–insensitive sulfide
175 disposal was relatively reduced compared to hepatocytes from C57BL/6J mice (Table S3).
176 Isolated liver mitochondria from *Tst*$^{-/-}$ hepatocytes also exhibited a higher sulfide disposal
177 rate (Table S3). In addition, cysteine and GSH was excreted at higher levels from *Tst*$^{-/-}$
178 hepatocytes under basal conditions and after stimulation of sulfur amino acid metabolism by
179 addition of methionine (Figure 2A and 2B). Consistent with higher GSH turnover, hepatocytes
180 from *Tst*$^{-/-}$ mice showed resistance to exogenous H_2O_2–mediated mitochondrial ROS
181 production (Figure S2). We next determined the global hepatic protein persulfidation profile,
182 the major post–translational modification mediated by sulfide[44–46]. Mass spectrometry

183 analysis of maleimide–labelled liver peptides revealed a greater abundance of peptides with
184 a lower persulfidation level (under-persulfidated) in the liver of *Tst*$^{-/-}$ mice (Figure 2C). We
185 confirmed this using semi-quantitative western–blot analysis on pulled down maleimide–
186 labelled proteins (Figure 2D). Gene Ontology (GO) analysis of proteins exhibiting altered
187 persulfidation levels revealed 28 terms different between *Tst*$^{-/-}$ and C57BL/6J mice by log–
188 fold change (Table 2). Major under-persulfidated terms (20) included "*FAD-binding*, *methyl*
189 *transferase, peroxisome, acyl-CoA dehydrogenase activity and transaminase*" while the less
190 abundant (8) over-persulfidated terms were dominated by terms related to "*Nicotinamide*
191 *metabolism*".

192 *The hepatic proteome of Tst*$^{-/-}$ *mice reveals a distinct molecular signature of altered sulfur*
193 *and mitochondrial nutrient metabolism.* To gain molecular insight into the mechanisms
194 underlying the apparently diabetogenic liver phenotype in ND-fed *Tst*$^{-/-}$ mice, we performed
195 a comparative iTRAQ proteomic analysis of whole liver with ND-fed C57BL/6J mice. Kyoto
196 Encyclopedia of Genes and Genomes (KEGG) analysis (at significance threshold $P < 0.05$)
197 revealed 4 up–regulated pathways in liver of *Tst*$^{-/-}$ mice related to amino acid metabolism,
198 including sulfur amino acids, and sulfur metabolism (Table 3A). GO analysis (at threshold $P <$
199 0.05) revealed 95 significantly up–regulated terms in liver of *Tst*$^{-/-}$ mice (Table S4A). Of the
200 top 14 up–regulated terms, 7 referred to amino acid metabolism and 1 referred to the
201 organellar term '*mitochondrion*'. KEGG pathway analysis revealed 27 down–regulated
202 pathways in the liver of *Tst*$^{-/-}$ mice (Table 3B) including Phase 1 and 2 detoxification
203 pathways (Cytochrome P450s, Glutathione and Glucuronidation) and '*Lysosome*', '*Protein*
204 *processing in the Endoplasmic reticulum'* organellar terms. 213 GO terms were significantly
205 down–regulated in *Tst*$^{-/-}$ mice (Table S4B). Among the most significant down–regulated
206 terms were phase 2 detoxification pathways such as *'glutathione binding'* and '*glutathione*

207 *transferase activity'* and '*endoplasmic reticulum'*. We validated a representative subset of
208 protein changes (Figures S3A), noting broadly consistent direction of change in the key
209 pathways. At the single protein level, the most robust change we observed was increased
210 MPST protein in whole liver (Figure S3A) and mitochondrial sub-fractions (Figure S3B). This
211 change was remarkable as mRNA levels for *Mpst* were lower in *Tst*$^{-/-}$ mice (Figure S3C), likely
212 as a result of loss of proximal *Mpst* promoter function; *Mpst* is a paralog of *Tst*[47] juxtaposed
213 approximately 1kb from *Tst*. Given the evidence for glucose and lipid metabolic changes in
214 the *Tst*$^{-/-}$ mice, we undertook a further focussed comparison of canonical proteins in these
215 pathways (Table S5). Four GO terms were enriched in liver from *Tst*$^{-/-}$ mice, all of which were
216 down–regulated; '*Lipid metabolic process'*, *'fatty acid beta-oxidation'*, *'Acyl-CoA*
217 *dehydrogenase activity' and 'Acyl-CoA hydrolase activity'* (Table S5).

218 *Hepatic protein expression in Tst*$^{-/-}$ *mice is consistent with lower NRF2 activation***.** We
219 performed a transcription factor binding site (TFBS) enrichment analysis in the promoters of
220 proteins that are up–regulated in the liver of *Tst*$^{-/-}$ mice to look for potential hub
221 transcriptional drivers of the proteome profile (Figure S4A). This revealed a statistically
222 significant under-representation of TFBS for the sulfide–responsive[48,49] NRF2 transcription
223 factor (Figure S4A). To explore whether there was evidence for reduced NRF2 activation in
224 the *Tst*$^{-/-}$ liver, we looked at the relative expression of 47 NRF2–regulated proteins in the
225 proteome of ND-fed *Tst*$^{-/-}$ and ND-fed C57Bl/6J mice. While 37 of these target proteins were
226 similar in expression between the genotypes, 10 NRF2 target proteins were lower in *Tst*$^{-/-}$
227 liver (Figure S4B) and none of the 47 NRF2 target proteins were increased in *Tst*$^{-/-}$ liver.

228 *Proteome of TST deficiency versus HFD response in C57BL/6J mice reveals distinct regulation*
229 *of lipid metabolism and detoxification pathways.* We examined mechanistic commonalities

230 between the diabetogenic hepatic phenotype of *Tst*$^{-/-}$ mice and that induced by the
231 diabetogenic HFD–feeding regimen in C57BL/6J mice. Note, ND-fed *Tst*$^{-/-}$ mice were in a pre-
232 existing diabetogenic state (Figure 1) that does not further worsen with HFD (Figure 1E-F,
233 Table S1B), suggesting gross phenotypic convergence of the two genotypes after HFD. We
234 compared the identity and direction of change of the 188 proteins differentially expressed in
235 ND-fed *Tst*$^{-/-}$ mice (versus ND-fed C57BL/6J mice; Figure 3A) to proteins that were
236 differentially expressed in response to HFD in C57BL/6J mice (432 proteins; Figure 3A). There
237 was a striking 67% overlap in individual proteins (126) in this comparison (Figure 3A). When
238 we analysed these two protein signatures for directionally shared pathways, one KEGG
239 pathway *'Glycine, serine and threonine metabolism'* was up–regulated (Table S6A) and 12
240 KEGG pathways were down–regulated, including *'drug metabolism'* and *'endoplasmic*
241 *reticulum'* (Table S6B). Consistent with a pre-existing HFD–like proteome, the proteomic
242 response in the liver of *Tst*$^{-/-}$ mice to HFD was muted, relative to that observed in C57BL6J
243 mice (106 proteins, a 4–fold lower response; Figure 3B). We then considered contrasting,
244 rather than congruent, proteomic responses arising from TST deficiency versus HFD responses
245 in C57BL/6J mice to illuminate potential novel pathways underlying the otherwise functionally
246 similar overall diabetogenic hepatic *Tst*$^{-/-}$ phenotype. 5 KEGG pathways (Table S7A) and 4
247 GO terms (Table S7B) were regulated in the opposite direction in this comparison. Strikingly,
248 the GO terms were all related to lipid metabolism, which were up–regulated in the HFD
249 response, but down–regulated with TST deficiency (Table S7A-B). An organelle–focussed
250 protein analysis showed shared up-regulation of mitochondrial and endoplasmic reticulum
251 pathways between TST deficiency (Figure 3C upper row) and C57BL/6J HFD-responses (Figure
252 3C lower row), but a striking discordance in peroxisomal protein pathways (up-regulated by

253 HFD, down-regulated TST deficiency) and nuclear proteins (down-regulated by HFD, up-
254 regulated TST deficiency; Figure 3C).

255 *The Tst$^{-/-}$ liver proteome and persulfidome converge on transamination and lipid oxidation*
256 *pathways.* To assess whether conservation of changes at protein and post-translational
257 modification levels can illuminate key regulatory hubs driving the hepatic phenotype we ran
258 a congruence analysis of the proteome and persulfidome. We found that GO terms referring
259 to amino acid, lipid metabolism and peroxisome were significantly regulated at both the level
260 of protein abundance and persulfidation status (Table 4).

261 *Tst$^{-/-}$ hepatocytes exhibit elevated mitochondrial respiration and a defect in medium–chain*
262 *fatty acid oxidation.* Enhanced respiratory sulfide disposal was found from *Tst$^{-/-}$*
263 hepatocytes, and enrichment of mitochondrial proteins was suggested from the liver
264 proteome of the *Tst$^{-/-}$* mice (Table S4). We therefore sought to determine if TST deficiency
265 affected respiratory function and substrate utilisation of the hepatocyte. Analysis of electron
266 micrographs prepared from the liver of ND-fed *Tst$^{-/-}$* mice and C57BL/6J controls showed
267 morphologically normal mitochondria (Figure 4A). Basal respiration, comprising ATP–linked
268 and leak respiration, was significantly higher in hepatocytes from *Tst$^{-/-}$* mice (Figure 4B–4D).
269 Maximal hepatocyte respiratory capacity and non–respiratory oxygen consumption was
270 similar between genotypes (Figures S5A and S5B). In line with phenotypic convergence
271 following HFD, hepatocyte respiration was comparable between genotypes from HFD-fed
272 mice (Figures S5C-S5H). A unique feature of the liver from *Tst$^{-/-}$* mice that contrasted with
273 HFD response in C57BL/6J mice was a decrease in proteins and persulfidation levels of
274 proteins in lipid oxidation pathways. We therefore investigated hepatocyte respiration of
275 lipids. Using a low pyruvate (100 μM) medium to reveal respiratory dependency on other

276 substrates, we showed that CPT1A–mediated mitochondrial oxidation of endogenous long
277 chain fatty acids (LCFA; etomoxir-inhibited) was similar between genotypes (Figure 4E). Next,
278 we by–passed CPT1A–mediated LCFA transfer, and revealed a marked deficit in respiration
279 stimulated by the medium chain fatty acid octanoate in hepatocytes from *Tst*$^{-/-}$ mice (Figure
280 4F). A similar experiment adding back pyruvate revealed comparable stimulation of
281 respiration between genotypes (Figure S5I). In amino acid free media, combined glutamine–,
282 aspartate– and alanine–stimulated hepatocyte respiration was comparable between
283 genotypes (Figure S5J).

284

285 # Discussion

286 Elevated TST expression in adipose tissue was recently identified as a genetic mechanism
287 driving metabolically protective leanness in mice[35]. Conversely, mice with genetic deletion of
288 *Tst* (*Tst*$^{-/-}$ mice) exhibited impaired glucose tolerance relative to C57BL/6N controls[35]. A key
289 observation from the *Tst*$^{-/-}$ mouse was qualitative evidence for elevated blood sulfide
290 levels[35], which implicated the mitochondrial sulfurtransferase in the breakdown of sulfide for
291 the first time *in vivo*. However, the mechanistic link between *Tst* deficiency and impaired
292 glucose tolerance remained unclear. The *Tst*$^{-/-}$ mice had a subtle adipose tissue phenotype,
293 with comparable fat accumulation upon high fat feeding, suggesting alternate organs as a
294 potential source of impaired glucose homeostasis. Moreover, TST is most highly abundant in
295 the liver, consistent with its role in detoxification of cyanide and related molecules. Indeed,
296 hepatic TST mRNA levels are ~8-fold higher than adipose tissue, with the difference in enzyme
297 activity likely substantially exceeding this, per gram of tissue. Based upon the reported effects
298 of sulfide to increase hepatic glucose production[20,21] and modulate lipid metabolism[22,23], we
299 hypothesised that TST deficiency predominantly drives a diabetogenic state through
300 increased hepatic sulfide exposure. Consistent with this, we found evidence for increased
301 gluconeogenesis, steatosis, elevated plasma VLDL triglycerides and, quantitatively, a 10-fold
302 higher circulating blood sulfide level in *Tst*$^{-/-}$ mice. Unexpectedly, and in spite of the
303 markedly increased circulating sulfide levels, steady-state sulfide level was normal in the liver
304 of *Tst*$^{-/-}$ mice. Moreover, we found evidence for multiple mechanisms for increased, not
305 decreased, hepatic sulfide disposal, reduced downstream sulfide signalling and novel
306 molecular explanations for the apparently diabetogenic phenotype. Our data are consistent
307 with the liver being a major site for sulfide disposal rather than production[32]. Moreover, our

308 data suggest that the liver of *Tst*$^{-/-}$ mice has over-compensated in its response to maximise
309 hepatic sulfide removal, thus engendering detrimental metabolic consequences indirectly.
310 This response is achieved through a combination of distinct compartmentalised cellular
311 responses including increased respiratory sulfide disposal and export of cysteine and GSH and
312 is further evidenced by the reduction of global hepatic protein persulfidation and depletion
313 of sulfide-responsive[49] NRF2 target proteins. Additionally, up-regulation of translation and
314 recruitment of MPST to the mitochondria of *Tst*$^{-/-}$ mice is observed. This response, in face
315 of reduced transcription of *Mpst* due to *Mpst* promoter disruption by the *Tst* null allele,
316 suggests a powerful post-transcriptional cellular sulfide sensing mechanism. Moreover, if
317 MPST is compensating for TST–mediated sulfide disposal in this context, this suggests a
318 subversion of normal MPST function away from sulfide production[50,51 52,53]. Intriguingly, TST
319 expression levels were elevated in the liver of *Mpst*$^{-/-}$ mice, providing further support for an
320 exquisite reciprocal compensatory mechanism between these two enzymes[54].
321 The unexpected finding of normal hepatic sulfide levels in the *Tst*$^{-/-}$ mice led us to discover
322 that the metabolic phenotype we observed was driven by the very mechanisms invoked to
323 maintain sulfide within a normal range rather than sulfide excess *per se*. Several observations
324 were consistent with this. For example, the major amino acid pathways increased in the liver
325 proteome of *Tst*$^{-/-}$ mice were transaminases involved in metabolism of GSH that support
326 increased export of sulfur equivalents as GSH (and cysteine). These same transaminases
327 support gluconeogenesis by redirecting Krebs cycle intermediates[55–57]. In addition,
328 glutathione-S-transferases (GST) that inhibit gluconeogenesis[58] were lower in the liver of *Tst*$^{-}$
329 $^{/-}$ mice. Further, NRF2 activation, which represses gluconeogenesis[59] appears lower in liver
330 of *Tst*$^{-/-}$ mice. The involvement of NRF2 in the *Tst*$^{-/-}$ liver phenotype is further supported by
331 the phenotype of *Nrf2*$^{-/-}$ mice that also exhibited steatohepatitis, in the absence of insulin

332 resistance[60]. However, we note that NRF2 signalling can be complex and dependent upon
333 dietary context; *Nrf2*$^{-/-}$ mice showed improved glucose tolerance after a high–fat diet[61]
334 suggesting any contribution of a NRF2 signalling deficit in the liver of the *Tst*$^{-/-}$ mice changes
335 upon high fat feeding. Beyond gluconeogenesis, we also showed that the hepatocytes of *Tst*$^{-}$
336 $^{/-}$ mice exhibited defective lipid metabolism. Specifically, medium–chain fatty acid (MCFA)
337 oxidation was impaired, associated with selective reduction of protein levels and
338 persulfidation levels of lipid catabolic enzymes. This represents a novel mechanism linking
339 altered sulfide metabolism to lipid oxidation, hepatic lipid accumulation and dyslipidaemia.
340 Consistent with impaired MCFA oxidation defects as a driver, at least in part, of the phenotype
341 of *Tst*$^{-/-}$ mice, steatosis is observed in medium–chain acyl-CoA dehydrogenase (*Mcad*)$^{-/-}$
342 mice[62] and dyslipidemia is found in MCADD deficient humans[63]. The data we present adds to
343 a growing understanding of the link between sulfide regulating genes and nutrient
344 metabolism that has hitherto focussed on the enzymes of sulfide production. Specifically, we
345 provide support for the importance of the sulfide oxidising pathway as a regulator of cellular
346 sulfide exposure. Unexpectedly, the data reveal novel cellular mechanisms that are engaged
347 to homeostatically regulate sulfide disposal and that can impact upon cell energetics and
348 nutrient metabolism.
349 Our findings may have implications for potentially unexpected side effects of sulfide donor
350 therapeutics. In normal mice, *in vivo* sulfide administration for 4 weeks post HFD partially
351 reversed hepatic lipid accumulation invoked by chronic (16 weeks) HFD[22]. No evidence was
352 provided for whether sulfide disposal mechanisms were altered[22]. This efficacious sub-
353 chronic sulfide administration regimen contrasts with our genetic model of chronic sulfide
354 elevation as a driver of dysregulated metabolism and NAFLD. Clearly, the normal mice in the
355 Na_2S administration studies had a fully functional SOP, suggesting the presence of TST is

356 required to achieve the beneficial metabolic effects of Na_2S administration. This is also
357 consistent with the apparently low sulfide signalling status (evidenced by lower
358 persulfidation, NRF2 target protein abundance) in the liver of the *Tst*$^{-/-}$ mice. The benefits
359 of elevated sulfide cannot be realised, perhaps because the major mediator of those effects
360 is missing and the alternate mechanisms invoked do not fully compensate (e.g. MPST) or
361 actively drive aberrant nutrient metabolism. Comparable studies of glucose and lipid
362 metabolism after manipulation of other sulfide regulating genes are limited. However in a
363 contrasting model of reduced sulfide production (*Cth*$^{-/-}$ mice), plasma triglycerides were
364 lowered[23], consistent and opposite to what we observed with the *Tst*$^{-/-}$ mice. The hepatic
365 sulfide disposal status of the *Cth*$^{-/-}$ mouse model is unknown, but our findings predict a
366 suppression of the SOP to spare the limited endogenous sulfide produced. Intriguingly they
367 also predict a knock-on effect on nutrient homeostasis due to reduced metabolic demand of
368 the TST/SOP axis. A more direct model informing on the effects of impairment of the sulfide
369 disposal pathway is deficiency of the key mitochondrial SOP enzyme ETHE1. *Ethe1*$^{-/-}$ mice
370 suffer fatal sulfide toxicity[30] and therefore comparable metabolic studies are lacking.
371 However, one notable observation is that *Ethe1*$^{-/-}$ mice have an apparently 10-fold higher
372 liver sulfide exposure than control mice[30], in contrast to the normalised hepatic sulfide levels
373 of *Tst*$^{-/-}$ mice. Circulating sulfide levels were not reported for comparison, but the
374 presumably relatively lower systemic sulfide levels of *Tst*$^{-/-}$ mice appear to have permitted
375 an effective homeostatic sulfide disposal response in the liver to avoid toxicity, albeit with a
376 metabolic cost. Consequently, the liver of *Tst*$^{-/-}$ mice has a distinct functional and proteomic
377 profile to that of the *Ethe1*$^{-/-}$ mice. For example, in the liver of *Tst*$^{-/-}$ and *Ethe1*$^{-/-}$ mice[64],
378 proteins of the glutathione–S–transferase Mu type (GSTM) and peroxiredoxin (PRDX) families
379 were altered, but sometimes in the opposite direction or with alteration of distinct protein

380 sub-classes. A notable difference is also observed in amino acid metabolism. The liver of
381 *Ethe1*$^{-/-}$ mice exhibited increased expression of enzymes of branched chain amino acid
382 metabolism[64], distinct from the predominantly glutathione–related amino acid pathways that
383 are increased in liver of *Tst*$^{-/-}$ mice. Beyond sulfide, TST may also have distinct cellular roles
384 that affect metabolism such as mitoribosomal synthesis, ROS attenuation and modulation of
385 mitochondrial iron-sulfur clusters[65–69].
386 Given the pro-diabetogenic liver phenotype in *Tst*$^{-/-}$ mice, its was surprising that insulin
387 signalling in the liver appeared normal, and peripheral insulin sensitivity was increased. There
388 are precedents for increased hepatic glucose production independent of insulin resistance, as
389 found in the *Nrf2*$^{-/-}$ mice[60] and as driven by the transcription factor ChREBP[70,71]. There is
390 also evidence to support insulin–sensitising effects of sulfide administration *in vivo* in mice
391 and rats[72–74], consistent with a sulfide–mediated insulin–sensitisation of non-hepatic tissues
392 in *Tst*$^{-/-}$ mice. Higher circulating GSH in *Tst*$^{-/-}$ mice may also promote peripheral insulin–
393 sensitisation[75,76]. Clearly, the net balance of glucose production from the liver and its
394 peripheral disposal remains abnormal in *Tst*$^{-/-}$ mice. Indeed, the baseline metabolic
395 phenotype of *Tst*$^{-/-}$ mice resembles in many ways that of a normal mouse fed a HFD. Thus
396 we expected to gain insight into conserved pro-diabetogenic mechanisms from the overlap
397 between the liver proteome of *Tst*$^{-/-}$ mice and that of HFD-fed C57BL/6J mice. However,
398 upon closer inspection this was not entirely the case, with some lipid metabolism and
399 peroxisomal proteins changing in the opposite direction to those observed in HFD–fed
400 C57BL/6J mice. Unlike a HFD state, which is associated with dominant hepatic insulin
401 resistance, the increased hepatic glucose production in ND-fed *Tst*$^{-/-}$ mice appears to be a
402 result of their over-compensated sulfide-removal response.

403 Sulfide donor therapeutics were proposed as a clinical strategy for improving cardiovascular
404 health[27,77,78]. Elevated endogenous sulfide was also implicated in the beneficial metabolic
405 effects of caloric restriction[11,79–83]. Our results suggest that chronic sulfide elevation may have
406 unintended detrimental consequences, driving liver glucose production and fat accumulation
407 to undesirable levels. This caveat may be fortunately limited to cases where SOP proteins are
408 compromised through rare genetic effects – such as TST variants[84,85]. More broadly, a number
409 of drugs or supplements are known to increase cyanide, which may dominantly inhibit TST
410 activity and result in secondary sulfide overexposure. These include nitroprusside[86] and
411 amygdalin[87,88]. Indeed the TST metabolite thiosulfate is commonly co-administered with
412 nitroprusside to prevent cyanide toxicity[89]. Furthermore, dietary and environmental exposure
413 to cyanogenic compounds[90], e.g. smoking[91] or cyanogenic diets[92] may interfere with normal
414 TST function and could lead to increased sensitivity to sulfide therapeutics. In contrast, we
415 have shown that administration of the TST substrate thiosulfate can ameliorate diabetes[35]
416 further underlining the potential utility of targeting the SOP in metabolic disease. As with all
417 therapeutic strategies, a careful cost-benefit analysis is required. A comparable case of
418 relevance are the statins, one of the most potent and widely used drugs to prevent
419 atherosclerosis, which also carry a higher risk for diabetes[93]. The full impact of TST
420 manipulation on opposing metabolic pathways requires further study. Our current study
421 sheds light on the underlying hepatic mechanisms invoked for sulfide disposal that are
422 relevant to current sulfide–donor strategines and may inform on routes to reduce their
423 potential metabolic side-effects.
424
425
426

Methods

The methods for all data and work presented in this manuscript is provided as supplementary information.

Author Contributions

N.M.M. and R.N.C conceived experiments. R.N.C., M.T.G.G, M. B.-L., A. M.-C., M.L., V.V., B.E., T. LeB., M.B., S.H., S.D., N.H., C. Mc F., A.T., N. F., T.G., performed experiments. R.N.C., M. B.-L., P.F., V.V., T. LeB., N.H., T.S., F.B., T.G., R.C.H., B.S., G.G., A.J.F., C.S., R.B. and N.M.M. analysed and interpreted data and commented on the manuscript. K.H.A., S.S. generated reagents. C.McM. and R.C.H. generated reagents. R.N.C. and N.M.M. wrote the manuscript.

Acknowledgements

This work was funded by a Wellcome Trust New Investigator Award to NMM (100981/Z/13/Z) and Diabetes UK grant (17/0005697). RCH was funded by a Medical Research Council Discovery Award (MC-PC-15076). We would like to thank Professor Ken Olsen and Eric DeLeon (Notre Dame) for advice establishing sulfide measurement by probe.

457 # References

458

459 1. OMS. GLOBAL REPORT ON DIABETES WHO Library Cataloguing-in-Publication Data.
460 *ISBN*. 2014;978:92-94. http://www.who.int/about/licensing/.
461 2. Lewis GF, Carpentier A, Adeli K, Giacca A. Disordered fat storage and mobilization in
462 the pathogenesis of insulin resistance and type 2 diabetes. *Endocr Rev*.
463 2002;23(2):201-229. doi:10.1210/edrv.23.2.0461
464 3. Consoli A, Nurjhan N, Capani F, Gerich J. Predominant role of gluconeogenesis in
465 increased hepatic glucose production in NIDDM. *Diabetes*. 1989;38(5):550-557.
466 doi:10.2337/diab.38.5.550
467 4. Caron S, Verrijken A, Mertens I, et al. Transcriptional activation of apolipoprotein CIII
468 expression by glucose may contribute to diabetic dyslipidemia. *Arterioscler Thromb*
469 *Vasc Biol*. 2011;31(3):513-519. doi:10.1161/ATVBAHA.110.220723
470 5. Abe K, Kimura H. The possible role of hydrogen sulfide as an endogenous
471 neuromodulator. *J Neurosci*. 1996;16(3):1066-1071.
472 http://www.ncbi.nlm.nih.gov/pubmed/8558235.
473 6. Wang R. Physiological Implications of Hydrogen Sulfide: A Whiff Exploration That
474 Blossomed. *Physiol Rev*. 2012;92(2):791-896. doi:10.1152/physrev.00017.2011
475 7. Mishanina T V., Libiad M, Banerjee R. Biogenesis of reactive sulfur species for
476 signaling by hydrogen sulfide oxidation pathways. *Nat Chem Biol*. 2015;11(7):457-
477 464. doi:10.1038/nchembio.1834
478 8. Filipovic MR, Zivanovic J, Alvarez B, Banerjee R. Chemical Biology of H_2S Signaling
479 through Persulfidation. *Chem Rev*. 2017. doi:10.1021/acs.chemrev.7b00205
480 9. Desai KM, Chang T, Untereiner A, Wu L. Hydrogen sulfide and the metabolic

481 syndrome. *Expert Rev Clin Pharmacol*. 2011;4(1):63-73. doi:10.1586/ecp.10.133
482 10. Szabo C. Roles of Hydrogen Sulfide in the Pathogenesis of Diabetes Mellitus and Its
483 Complications. *Antioxid Redox Signal*. 2011;17(1):68-80. doi:10.1089/ars.2011.4451
484 11. Hine C, Harputlugil E, Zhang Y, et al. Endogenous hydrogen sulfide production is
485 essential for dietary restriction benefits. *Cell*. 2015. doi:10.1016/j.cell.2014.11.048
486 12. Carter RN, Morton NM. Cysteine and hydrogen sulphide in the regulation of
487 metabolism: Insights from genetics and pharmacology. *J Pathol*. 2016;238(2):321-332.
488 doi:10.1002/path.4659
489 13. Chen X, Jhee KH, Kruger WD. Production of the neuromodulator H2S by
490 cystathionine ??-synthase via the condensation of cysteine and homocysteine. *J Biol*
491 *Chem*. 2004. doi:10.1074/jbc.C400481200
492 14. Singh S, Padovani D, Leslie RA, Chiku T, Banerjee R. Relative contributions of
493 cystathionine ??-synthase and ??-cystathionase to H2S biogenesis via alternative
494 trans-sulfuration reactions. *J Biol Chem*. 2009. doi:10.1074/jbc.M109.010868
495 15. Shibuya N, Tanaka M, Yoshida M, et al. 3-Mercaptopyruvate Sulfurtransferase
496 Produces Hydrogen Sulfide and Bound Sulfane Sulfur in the Brain. *Antioxid Redox*
497 *Signal*. 2009. doi:10.1089/ars.2008.2253
498 16. Mikami Y, Shibuya N, Kimura Y, Nagahara N, Ogasawara Y, Kimura H. Thioredoxin and
499 dihydrolipoic acid are required for 3-mercaptopyruvate sulfurtransferase to produce
500 hydrogen sulfide. *Biochem J*. 2011. doi:10.1042/BJ20110841
501 17. Yadav PK, Yamada K, Chiku T, Koutmos M, Banerjee R. Structure and kinetic analysis
502 of H2S production by human mercaptopyruvate sulfurtransferase. *J Biol Chem*. 2013.
503 doi:10.1074/jbc.M113.466177
504 18. Wedmann R, Onderka C, Wei S, et al. Improved tag-switch method reveals that

505 thioredoxin acts as depersulfidase and controls the intracellular levels of protein
506 persulfidation. *Chem Sci*. 2016;7(5):3414-3426. doi:10.1039/c5sc04818d
507 19. Mani S, Cao W, Wu L, Wang R. Hydrogen sulfide and the liver. *Nitric Oxide - Biol*
508 *Chem*. 2014. doi:10.1016/j.niox.2014.02.006
509 20. Pichette J, Gagnon J. Implications of Hydrogen Sulfide in Glucose Regulation: How
510 H2S Can Alter Glucose Homeostasis through Metabolic Hormones. *Oxid Med Cell*
511 *Longev*. 2016;2016. doi:10.1155/2016/3285074
512 21. Zhang L, Yang G, Untereiner A, Ju Y, Wu L, Wang R. Hydrogen sulfide impairs glucose
513 utilization and increases gluconeogenesis in hepatocytes. *Endocrinology*. 2013.
514 doi:10.1210/en.2012-1658
515 22. Wu D, Zheng N, Qi K, et al. Exogenous hydrogen sulfide mitigates the fatty liver in
516 obese mice through improving lipid metabolism and antioxidant potential. *Med Gas*
517 *Res*. 2015;5(1). doi:10.1186/s13618-014-0022-y
518 23. Mani S, Li H, Untereiner A, et al. Decreased endogenous production of hydrogen
519 sulfide accelerates atherosclerosis. *Circulation*. 2013;127(25):2523-2534.
520 doi:10.1161/CIRCULATIONAHA.113.002208
521 24. Distrutti E, Mencarelli A, Santucci L, et al. The methionine connection: Homocysteine
522 and hydrogen sulfide exert opposite effects on hepatic microcirculation in rats.
523 *Hepatology*. 2008;47(2):659-667. doi:10.1002/hep.22037
524 25. Fiorucci S, Antonelli E, Mencarelli A, et al. The third gas: H2S regulates perfusion
525 pressure in both the isolated and perfused normal rat liver and in cirrhosis.
526 *Hepatology*. 2005;42(3):539-548. doi:10.1002/hep.20817
527 26. Sestito S, Nesi G, Pi R, Macchia M, Rapposelli S. Hydrogen Sulfide: A Worthwhile Tool
528 in the Design of New Multitarget Drugs. *Front Chem*. 2017;5.

529 doi:10.3389/fchem.2017.00072

530 27. Whiteman M, Le Trionnaire S, Chopra M, Fox B, Whatmore J. Emerging role of
531 hydrogen sulfide in health and disease: critical appraisal of biomarkers and
532 pharmacological tools. *Clin Sci*. 2011;121(11):459-488. doi:10.1042/cs20110267

533 28. Libiad M, Motl N, Akey DL, et al. Thiosulfate Sulfurtransferase like Domain Containing
534 1 Protein Interacts with Thioredoxin. *J Biol Chem*. January 2018:jbc.RA117.000826.
535 doi:10.1074/jbc.RA117.000826

536 29. Reiffenstein R. Toxicology Of Hydrogen Sulfide. *Annu Rev Pharmacol Toxicol*.
537 1992;32(1):109-134. doi:10.1146/annurev.pharmtox.32.1.109

538 30. Tiranti V, Viscomi C, Hildebrandt T, et al. Loss of ETHE1, a mitochondrial dioxygenase,
539 causes fatal sulfide toxicity in ethylmalonic encephalopathy. *Nat Med*.
540 2009;15(2):200-205. doi:10.1038/nm.1907

541 31. Hildebrandt TM, Grieshaber MK. Three enzymatic activities catalyze the oxidation of
542 sulfide to thiosulfate in mammalian and invertebrate mitochondria. *FEBS J*.
543 2008;275(13):3352-3361. doi:10.1111/j.1742-4658.2008.06482.x

544 32. Norris EJ, Culberson CR, Narasimhan S, Clemens MG. The liver as a central regulator
545 of hydrogen sulfide. *Shock*. 2011. doi:10.1097/SHK.0b013e3182252ee7

546 33. Jackson MR, Melideo SL, Jorns MS. Human sulfide:Quinone oxidoreductase catalyzes
547 the first step in hydrogen sulfide metabolism and produces a sulfane sulfur
548 metabolite. *Biochemistry*. 2012. doi:10.1021/bi300778t

549 34. Libiad M, Yadav PK, Vitvitsky V, Martinov M, Banerjee R. Organization of the human
550 mitochondrial hydrogen sulfide oxidation pathway. *J Biol Chem*. 2014.
551 doi:10.1074/jbc.M114.602664

552 35. Morton NM, Beltram J, Carter RN, et al. Genetic identification of thiosulfate

553 sulfurtransferase as an adipocyte-expressed antidiabetic target in mice selected for
554 leanness. *Nat Med*. 2016;22(7). doi:10.1038/nm.4115
555 36. Gero, Domokos Torregrossa R, Perry A, Waters A, et al. The novel mitochondria-
556 targeted hydrogen sulfide (H2S) donors AP123 and AP39 protect against
557 hyperglycemic injury in microvascular endothelial cells in vitro. *Pharmacol Res*.
558 2016;113:186-198.
559 https://reader.elsevier.com/reader/sd/pii/S1043661816306314?token=3623BE15023
560 42420421E3956873F1E65FD3FCBDE1D675D7396DB26A…1/13.
561 37. Karwi QG, Bice JS, Baxter GF. Pre- and postconditioning the heart with hydrogen
562 sulfide (H2S) against ischemia/reperfusion injury in vivo: a systematic review and
563 meta-analysis. *Basic Res Cardiol*. 2018;113(1). doi:10.1007/s00395-017-0664-8
564 38. Mason TM. The role of factors that regulate the synthesis and secretion of very-low-
565 density lipoprotein by hepatocytes. *Crit Rev Clin Lab Sci*. 1998;35(6):461-487.
566 doi:10.1080/10408369891234246
567 39. Vitvitsky V, Yadav PK, Kurthen A, Banerjee R. Sulfide oxidation by a noncanonical
568 pathway in red blood cells generates thiosulfate and polysulfides. *J Biol Chem*.
569 2015;290(13):8310-8320. doi:10.1074/jbc.M115.639831
570 40. Vitvitsky V, Yadav PK, An S, Seravalli J, Cho US, Banerjee R. Structural and mechanistic
571 insights into hemoglobincatalyzed hydrogen sulfide oxidation and the fate of
572 polysulfide products. *J Biol Chem*. 2017. doi:10.1074/jbc.M117.774943
573 41. Banerjee R, Chiku T, Kabil O, Libiad M, Motl N, Yadav PK. *Assay Methods for H2S*
574 *Biogenesis and Catabolism Enzymes*. Vol 554. Academic Press Inc.; 2015:189-200.
575 doi:10.1016/bs.mie.2014.11.016
576 42. Singha S, Kim D, Moon H, et al. Toward a selective, sensitive, fast-responsive, and

577 biocompatible two-photon probe for hydrogen sulfide in live cells. *Anal Chem*.
578 2015;87(2):1188-1195. doi:10.1021/ac503806w
579 43. Arndt S, Baeza-Garza CD, Logan A, et al. Assessment of H 2 S in vivo using the newly
580 developed mitochondria-targeted mass spectrometry probe MitoA. *J Biol Chem*.
581 2017;292(19):7761-7773. doi:10.1074/jbc.M117.784678
582 44. Krishnan N, Fu C, Pappin DJ, Tonks NK. H2S-Induced Sulfhydration of the Phosphatase
583 PTP1B and Its Role in the Endoplasmic Reticulum Stress Response. *Sci Signal*. 2011.
584 doi:10.1126/scisignal.2002329
585 45. Kabil O, Motl N, Banerjee R. H2S and its role in redox signaling. *Biochim Biophys Acta -*
586 *Proteins Proteomics*. 2014;1844(8):1355-1366. doi:10.1016/j.bbapap.2014.01.002
587 46. Koike S, Nishimoto S, Ogasawara Y. Cysteine persulfides and polysulfides produced by
588 exchange reactions with H2S protect SH-SY5Y cells from methylglyoxal-induced
589 toxicity through Nrf2 activation. *Redox Biol*. 2017;12:530-539.
590 doi:10.1016/j.redox.2017.03.020
591 47. Nagahara N. Catalytic Site Cysteines of Thiol Enzyme: Sulfurtransferases. *J Amino*
592 *Acids*. 2011. doi:10.4061/2011/709404
593 48. Xie L, Gu Y, Wen M, et al. Hydrogen sulfide induces Keap1 S-sulfhydration and
594 suppresses diabetes-accelerated atherosclerosis via Nrf2 activation. *Diabetes*.
595 2016;65(10):3171-3184. doi:10.2337/db16-0020
596 49. Yang G, Zhao K, Ju Y, et al. Hydrogen sulfide protects against cellular senescence via s-
597 sulfhydration of keap1 and activation of Nrf2. *Antioxidants Redox Signal*.
598 2013;18(15):1906-1919. doi:10.1089/ars.2012.4645
599 50. Módis K, Coletta C, Erdélyi K, Papapetropoulos A, Szabo C. Intramitochondrial
600 hydrogen sulfide production by 3-mercaptopyruvate sulfurtransferase maintains

601 mitochondrial electron flow and supports cellular bioenergetics. *FASEB J*. 2013.
602 doi:10.1096/fj.12-216507
603 51. Szabo C, Ransy C, Módis K, et al. Regulation of mitochondrial bioenergetic function by
604 hydrogen sulfide. Part I. Biochemical and physiological mechanisms. *Br J Pharmacol*.
605 2014. doi:10.1111/bph.12369
606 52. Nagahara N. Multiple role of 3-mercaptopyruvate sulfurtransferase: antioxidative
607 function, H2S and polysulfide production and possible SOx production. *Br J*
608 *Pharmacol*. 2018;175(4):577-589. doi:10.1111/bph.14100
609 53. Kimura Y, Koike S, Shibuya N, Lefer D, Ogasawara Y, Kimura H. 3-Mercaptopyruvate
610 sulfurtransferase produces potential redox regulators cysteine- and glutathione-
611 persulfide (Cys-SSH and GSSH) together with signaling molecules H 2 S 2 , H 2 S 3 and
612 H 2 S. *Sci Rep*. 2017;7(1):1-14. doi:10.1038/s41598-017-11004-7
613 54. Nagahara N, Tanaka M, Tanaka Y, Ito T. Novel Characterization of Antioxidant
614 Enzyme, 3-Mercaptopyruvate Sulfurtransferase-Knockout Mice: Overexpression of
615 the Evolutionarily-Related Enzyme Rhodanese. *Antioxidants*. 2019;8(5):116.
616 doi:10.3390/antiox8050116
617 55. Rui L. Energy metabolism in the liver. *Compr Physiol*. 2014;4(1):177-197.
618 doi:10.1002/cphy.c130024
619 56. Qian K, Zhong S, Xie K, Yu D, Yang R, Gong DW. Hepatic ALT isoenzymes are elevated
620 in gluconeogenic conditions including diabetes and suppressed by insulin at the
621 protein level. *Diabetes Metab Res Rev*. 2015;31(6):562-571. doi:10.1002/dmrr.2655
622 57. Sookoian S, Castaño GO, Scian R, et al. Serum aminotransferases in nonalcoholic fatty
623 liver disease are a signature of liver metabolic perturbations at the amino acid and
624 Krebs cycle level. *Am J Clin Nutr*. 2016;103(2):422-434. doi:10.3945/ajcn.115.118695

625 58. Ghosh Dastidar S, Jagatheesan G, Haberzettl P, et al. Glutathione S -transferase P
626 deficiency induces glucose intolerance via JNK-dependent enhancement of hepatic
627 gluconeogenesis . *Am J Physiol Metab*. 2018;315(5):E1005-E1018.
628 doi:10.1152/ajpendo.00345.2017
629 59. Slocum SL, Skoko JJ, Wakabayashi N, et al. Keap1/Nrf2 pathway activation leads to a
630 repressed hepatic gluconeogenic and lipogenic program in mice on a high-fat diet.
631 *Arch Biochem Biophys*. 2016;591:57-65. doi:10.1016/j.abb.2015.11.040
632 60. Meakin PJ, Chowdhry S, Sharma RS, et al. Susceptibility of Nrf2-Null Mice to
633 Steatohepatitis and Cirrhosis upon Consumption of a High-Fat Diet Is Associated with
634 Oxidative Stress, Perturbation of the Unfolded Protein Response, and Disturbance in
635 the Expression of Metabolic Enzymes but Not with Insulin Resistance. *Mol Cell Biol*.
636 2014;34(17):3305-3320. doi:10.1128/mcb.00677-14
637 61. Zhang YKJ, Wu KC, Liu J, Klaassen CD. Nrf2 deficiency improves glucose tolerance in
638 mice fed a high-fat diet. *Toxicol Appl Pharmacol*. 2012;264(3):305-314.
639 doi:10.1016/j.taap.2012.09.014
640 62. Tolwani RJ, Hamm DA, Tian L, et al. Medium-chain acyl-CoA dehydrogenase deficiency
641 in gene-targeted mice. *PLoS Genet*. 2005;1(2):0205-0212.
642 doi:10.1371/journal.pgen.0010023
643 63. Onkenhout W, Venizelos V, Van Der Poet PFH, Van Den Heuvel MPM, Poorthuis
644 BJHM. *Identification and Quantification of Intermediates of Unsaturated Fatty Acid*
645 *Metabolism in Plasma of Patients with Fatty Acid Oxidation Disorders*. Vol 10.; 1995.
646 64. Hildebrandt TM, Di Meo I, Zeviani M, Viscomi C, Braun H. Proteome adaptations in
647 Ethe1-deficient mice indicate a role in lipid catabolism and cytoskeleton organization
648 via post-translational protein modifications. *Biosci Rep*. 2013;33(4):575-584.

649 doi:10.1042/bsr20130051

650 65. Bonomi F, Pagani S, Cerletti P, Cannella C. *Rhodanese-Mediated Sulfur Transfer to*
651 *Succinate Dehydrogenase*. Vol 72.; 1977.

652 66. Pagan1 S, Galante YM. *INTERACTION OF RHODANESE WITH MITOCHONDRIAL NADH*
653 *DEHYDROGENASE*. Vol 742.; 1983.

654 67. Nandi DL, Westley J. Reduced thioredoxin as a sulfur-acceptor substrate for
655 rhodanese. *Int J Biochem Cell Biol*. 1998. doi:10.1016/S1357-2725(98)00050-8

656 68. Nandi DL, Horowitz PM, Westley J. Rhodanese as a thioredoxin oxidase. *Int J Biochem*
657 *Cell Biol*. 2000;32(4):465-473. doi:10.1016/S1357-2725(99)00035-7

658 69. Smirnov A, Comte C, Mager-Heckel AM, et al. Mitochondrial enzyme rhodanese is
659 essential for 5 S ribosomal RNA import into human mitochondria. *J Biol Chem*.
660 2010;285(40):30792-30803. doi:10.1074/jbc.M110.151183

661 70. Uyeda K, Repa JJ. Carbohydrate response element binding protein, ChREBP, a
662 transcription factor coupling hepatic glucose utilization and lipid synthesis. *Cell*
663 *Metab*. 2006;4(2):107-110. doi:10.1016/j.cmet.2006.06.008

664 71. Kim MS, Krawczyk SA, Doridot L, et al. ChREBP regulates fructose-induced glucose
665 production independently of insulin signaling. *J Clin Invest*. 2016;126(11):4372-4386.
666 doi:10.1172/JCI81993

667 72. Xue R, Hao D-D, Sun J-P, et al. Hydrogen Sulfide Treatment Promotes Glucose Uptake
668 by Increasing Insulin Receptor Sensitivity and Ameliorates Kidney Lesions in Type 2
669 Diabetes. *Antioxid Redox Signal*. 2013;19(1):5-23. doi:10.1089/ars.2012.5024

670 73. Feng X, Chen Y, Zhao J, Tang C, Jiang Z, Geng B. Hydrogen sulfide from adipose tissue
671 is a novel insulin resistance regulator. *Biochem Biophys Res Commun*. 2009.
672 doi:10.1016/j.bbrc.2009.01.059

673 74. Geng B, Cai B, Liao F, et al. Increase or Decrease Hydrogen Sulfide Exert Opposite
674 Lipolysis, but Reduce Global Insulin Resistance in High Fatty Diet Induced Obese Mice.
675 *PLoS One*. 2013;8(9). doi:10.1371/journal.pone.0073892
676 75. Lutchmansingh FK, Hsu JW, Bennett FI, et al. Glutathione metabolism in type 2
677 diabetes and its relationship with microvascular complications and glycemia. *PLoS*
678 *One*. 2018;13(6). doi:10.1371/journal.pone.0198626
679 76. Jain SK, Micinski D, Huning L, Kahlon G, Bass PF, Levine SN. Vitamin D and L-cysteine
680 levels correlate positively with GSH and negatively with insulin resistance levels in the
681 blood of type 2 diabetic patients. *Eur J Clin Nutr*. 2014;68(10):1148-1153.
682 doi:10.1038/ejcn.2014.114
683 77. Zhang L, Wang Y, Li Y, et al. Hydrogen sulfide (H2S)-releasing compounds: Therapeutic
684 potential in cardiovascular diseases. *Front Pharmacol*. 2018;9(SEP).
685 doi:10.3389/fphar.2018.01066
686 78. Szabó G, Veres G, Radovits T, et al. Cardioprotective effects of hydrogen sulfide. In:
687 *Nitric Oxide - Biology and Chemistry*. Vol 25. ; 2011:201-210.
688 doi:10.1016/j.niox.2010.11.001
689 79. Miller RA, Buehner G, Chang Y, Harper JM, Sigler R, Smith-Wheelock M. Methionine-
690 deficient diet extends mouse lifespan, slows immune and lens aging, alters glucose,
691 T4, IGF-I and insulin levels, and increases hepatocyte MIF levels and stress resistance.
692 *Aging Cell*. 2005. doi:10.1111/j.1474-9726.2005.00152.x
693 80. Lee BC, Kaya A, Gladyshev VN. Methionine restriction and life-span control. *Ann N Y*
694 *Acad Sci*. 2016. doi:10.1111/nyas.12973
695 81. Shimokawa I, Komatsu T, Hayashi N, et al. The life-extending effect of dietary
696 restriction requires Foxo3 in mice. *Aging Cell*. 2015. doi:10.1111/acel.12340

697 82. Hine C, Kim HJ, Zhu Y, et al. Hypothalamic-Pituitary Axis Regulates Hydrogen Sulfide
698 Production. *Cell Metab*. 2017. doi:10.1016/j.cmet.2017.05.003
699 83. Hine C, Zhu Y, Hollenberg AN, Mitchell JR. Dietary and Endocrine Regulation of
700 Endogenous Hydrogen Sulfide Production: Implications for Longevity. *Antioxid Redox*
701 *Signal*. 2018;28(16):1483-1502. doi:10.1089/ars.2017.7434
702 84. Libiad M, Sriraman A, Banerjee R. Polymorphic variants of human rhodanese exhibit
703 differences in thermal stability and sulfur transfer kinetics. *J Biol Chem*. 2015.
704 doi:10.1074/jbc.M115.675694
705 85. Billaut-Laden I, Allorge D, Crunelle-Thibaut A, et al. Evidence for a functional genetic
706 polymorphism of the human thiosulfate sulfurtransferase (Rhodanese), a cyanide and
707 H2S detoxification enzyme. *Toxicology*. 2006;225(1):1-11.
708 doi:10.1016/j.tox.2006.04.054
709 86. Morris AA, Page RL, Baumgartner LJ, et al. Thiocyanate Accumulation in Critically Ill
710 Patients Receiving Nitroprusside Infusions. *J Intensive Care Med*. 2017;32(9):547-553.
711 doi:10.1177/0885066616657004
712 87. Bromley J, Hughes BGM, Leong DCS, Buckley NA. Life-threatening interaction
713 between complementary medicines: Cyanide toxicity following ingestion of
714 amygdalin and vitamin C. *Ann Pharmacother*. 2005;39(9):1566-1569.
715 doi:10.1345/aph.1E634
716 88. O'brien B, Quigg C, Leong T. *Severe Cyanide Toxicity from "Vitamin Supplements."* Vol
717 12. Lippincott Williams & Wilkins; 2005.
718 http://www.cancer.gov/cancerinfo/pdq/cam.laetrile.
719 89. Curry SC, Carlton MW, Raschke RA. Prevention of fetal and maternal cyanide toxicity
720 from nitroprusside with coinfusion of sodium thiosulfate in gravid ewes. *Anesth*

Analg. 1997;84(5):1121-1126. doi:10.1213/00000539-199705000-00031

90. Petrova F. Hydrogen cyanide and cyanides : human health aspects. 2004:67.

91. Vinnakota C V., Peetha NS, Perrizo MG, et al. Comparison of cyanide exposure markers in the biofluids of smokers and non-smokers. *Biomarkers*. 2012;17(7):625-633. doi:10.3109/1354750X.2012.709880

92. Kashala-Abotnes E, Okitundu D, Mumba D, Boivin MJ, Tylleskär T, Tshala-Katumbay D. Konzo: a distinct neurological disease associated with food (cassava) cyanogenic poisoning. *Brain Res Bull*. 2019;145:87-91. doi:10.1016/j.brainresbull.2018.07.001

93. Swerdlow DI, Preiss D, Kuchenbaecker KB, et al. HMG-coenzyme A reductase inhibition, type 2 diabetes, and bodyweight: Evidence from genetic analysis and randomised trials. *Lancet*. 2015;385(9965):351-361. doi:10.1016/S0140-6736(14)61183-1

745 # Figures and Legends

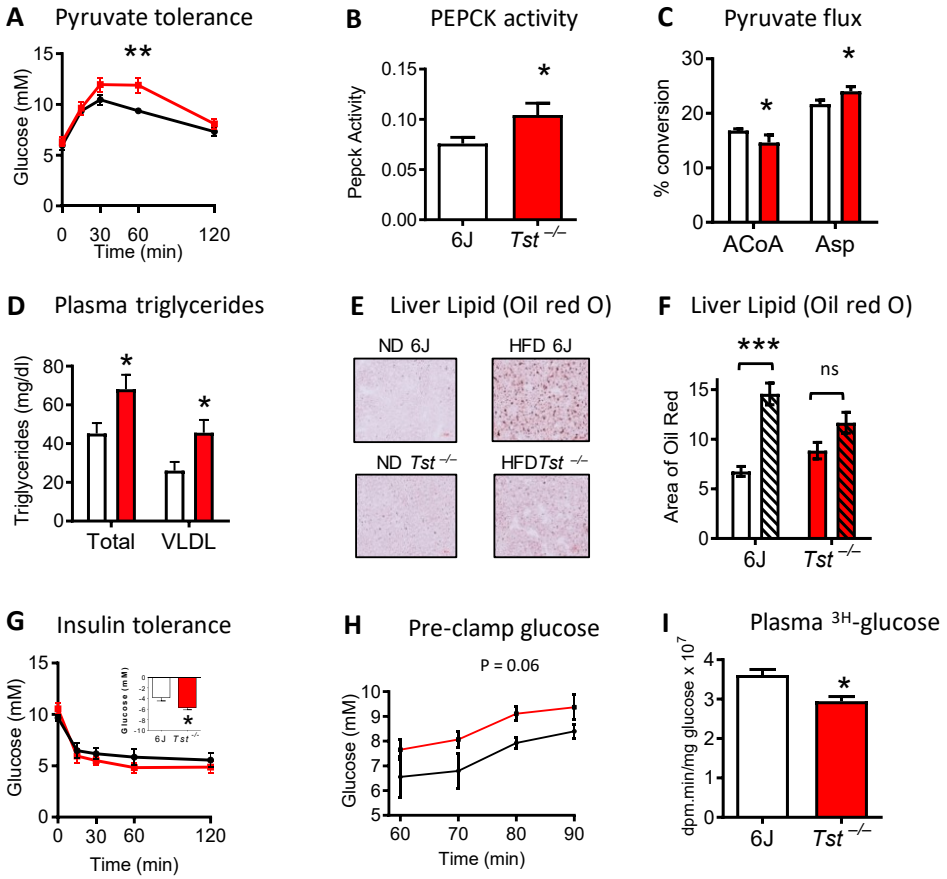

746 **Figure 1. *Tst* deletion results in impaired glucose and lipid metabolism.** (**A**) Plasma glucose over 120
747 minutes, following pyruvate (i.p., 1.5mg/g) administration in overnight fasted C57Bl/6J (black line, n =
748 9) and *Tst*$^{-/-}$ (red line, n = 8) normal diet-fed mice. (**B**) Extinction of NADH measured by absorbance
749 at 340nm, coupled to PEPCK activity from liver homogenates taken from C57Bl/6J (white bar, n = 6)
750 and *Tst*$^{-/-}$ (red bar, n = 6) normal diet-fed mice. (**C**) Production of ^{13}C (M+2) acetyl-CoA and ^{13}C (M+3)
751 aspartate generated from 3-carbon labelled ^{13}C (M+3) pyruvate, expressed as a percentage of the total
752 amount of detected metabolite, in primary hepatocytes from C57Bl/6J (white bars, n = 6) and *Tst*$^{-/-}$
753 (red bars, n = 5) normal diet-fed mice. (**D**) HPLC quantified total and VLDL plasma triglyceride in 4 hour
754 fasted C57Bl/6J (white bar, n = 6), and *Tst*$^{-/-}$ (red bar, n = 6) normal diet-fed mice. (**E**) Representative
755 light microscopic images of fixed liver stained with Oil-Red O from normal diet-fed (ND) or high fat
756 diet-fed (HFD) C57Bl/6J and *Tst*$^{-/-}$ mice. (**F**) Analysis of the area of red staining (Oil Red O) after
757 thresholding, using Image J, from normal diet-fed (no pattern, n = 3-4/genotype) or high fat diet-fed
758 (hatched pattern, n = 4-5/genotype) C57Bl/6J (white bars) and *Tst*$^{-/-}$ (red bars) mice. (**G**) Plasma
759 glucose over 120 minutes following insulin (i.p., 1mU/g) administration in 4 hour fasted C57Bl/6J
760 (black line, n = 8) and *Tst*$^{-/-}$(red line, n = 7) normal diet-fed mice. Inset; Reduction in plasma glucose
761 from baseline levels 60 minutes after the injection of insulin. (**H**) Blood glucose during the pre-clamp
762 phase of the hyperinsulinemic, euglycaemic clamp from C57Bl/6J (white, n = 3), and *Tst*$^{-/-}$ (red, n =
763 6) normal diet-fed mice. Significance is reported from area under curve analysis. (**I**) Mean integrated
764 radioactive glucose (inversely related to whole body glucose uptake) during a hyperinsulinemic,
765 euglycaemic clamp from normal diet fed C57Bl/6J control (white, n = 3), and *Tst*$^{-/-}$ (red, n = 6) mice.
766 Data are represented as mean ±SEM. Significance was calculated using repeated measures ANOVA
767 (**A**,**G**) 2-WAY ANOVA (**C**,**F**) or unpaired two-tailed student's t-test (**B**,**D**,**H**,**I**) * $P < 0.05$, ** $P < 0.01$. For
768 (**C**) the 2-WAY ANOVA revealed no overall effect of genotype, however a significant interaction
769 between metabolite and genotype was found. The * on the histogram represents this interaction. For
770 (**F**) no main genotype effect was found, but a significant effect of diet, and an interaction were found.
771 Post Hoc analysis using Sidaks' multiple comparison test show an effect of diet on the 6J controls (***),
772 whereas no effect of diet is found on the *Tst*$^{-/-}$.

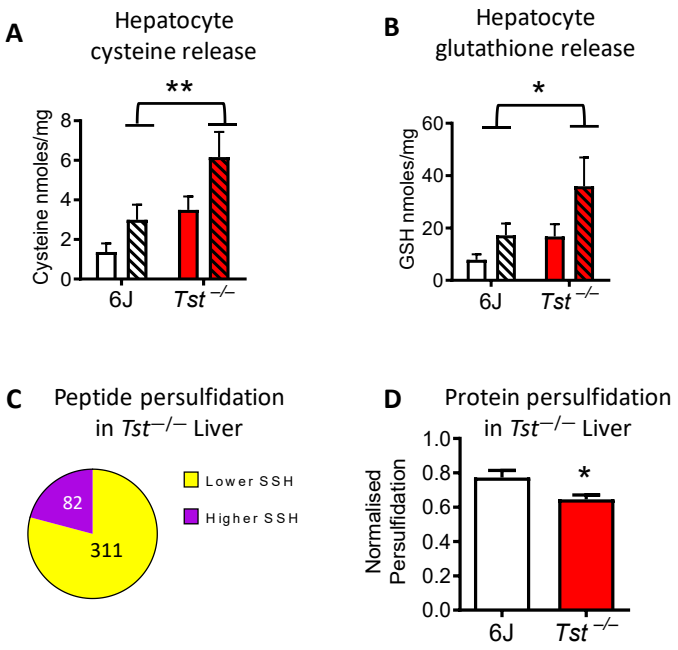

Figure 2. *Tst* deletion results in increased hepatic sulfur excretion and a reduction of protein persulfidation. (**A**) Cysteine concentrations (MBB-HPLC) in the media incubated with primary hepatocytes in the presence (hatched pattern) or absence (no pattern) of 1mM methionine, from C57Bl/6J (white bars, n = 4/treatment) and *Tst*$^{-/-}$ (red bars, n = 4/treatment) mice. (**B**) Glutathione concentrations (MBB-HPLC) in the media incubated with primary hepatocytes in the presence (hatched pattern) or absence (no pattern) of 1mM methionine, from C57Bl/6J (white bars, n = 4/treatment) and *Tst*$^{-/-}$ (red bars, n = 4/treatment) mice. (**C**) Pie chart depicting the proportion of liver peptides that are significantly higher (82 peptides, purple space) or lower (311 peptides, yellow space), in their persulfidation rate in the *Tst*$^{-/-}$ (n = 3) relative to C57Bl/6J (n = 3) mice. (**D**) Total DTT-released cysteine-persulfidated liver protein as measured by REVERT total protein stain following western blotting, normalised to the total input protein of the sample from *Tst*$^{-/-}$ (red bar, n = 4) and C57Bl/6J (white bar, n = 4) mice. Data with error bars are represented as mean ±SEM. Significance was calculated using 2-WAY ANOVA (**A**, **B**) or student's t-test (**D**), * $P < 0.05$, ** $P < 0.01$. For (**A**) and (**B**) the 2-WAY ANOVA reveals a main effect of genotype, indicated by * or ** on the histogram. A significant effect of methionine was also found for both (**A**) and (**B**) not indicated on the histogram. For (**C**) peptides were selected as being significant at a P-diff of 0.95 or greater.

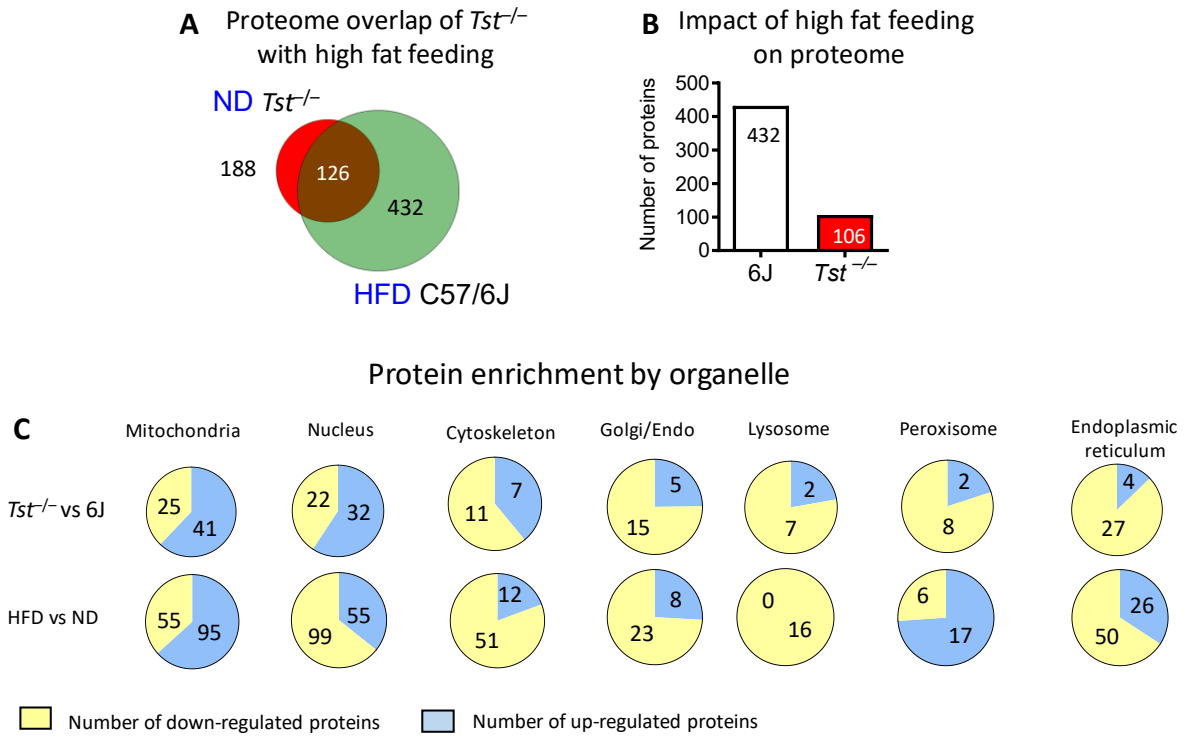

Figure 3. *Tst* deletion engenders a high fat feeding–like hepatic proteome with a distinct organellar signature. (**A**) Venn diagram representing the number of proteins significantly different (at P < 0.01) between normal diet-fed *Tst*$^{-/-}$ and C57Bl/6J (Red circle), and the number of regulated proteins between high fat fed and normal diet-fed C57Bl/6J (Green circle). The overlap (brown) represents those proteins regulated in the same direction by both comparisons (n= 4/genotype). (**B**) Number of proteins significantly different (at p < 0.01) between 58% high fat and normal diet in either C57Bl/6J (white bar), or *Tst*$^{-/-}$ mice (Red bar), (n= 4/genotype). (**C**) Pie charts depicting the proportion of individual liver proteins that are upregulated (Blue space) compared to downregulated (yellow space) after GO term categorisation according to subcellular location. Upper row; normal diet-fed *Tst*$^{-/-}$ relative to normal diet-fed C57Bl/6J. Lower row, high fat-fed C57Bl/6J relative to normal diet-fed C57Bl/6J.

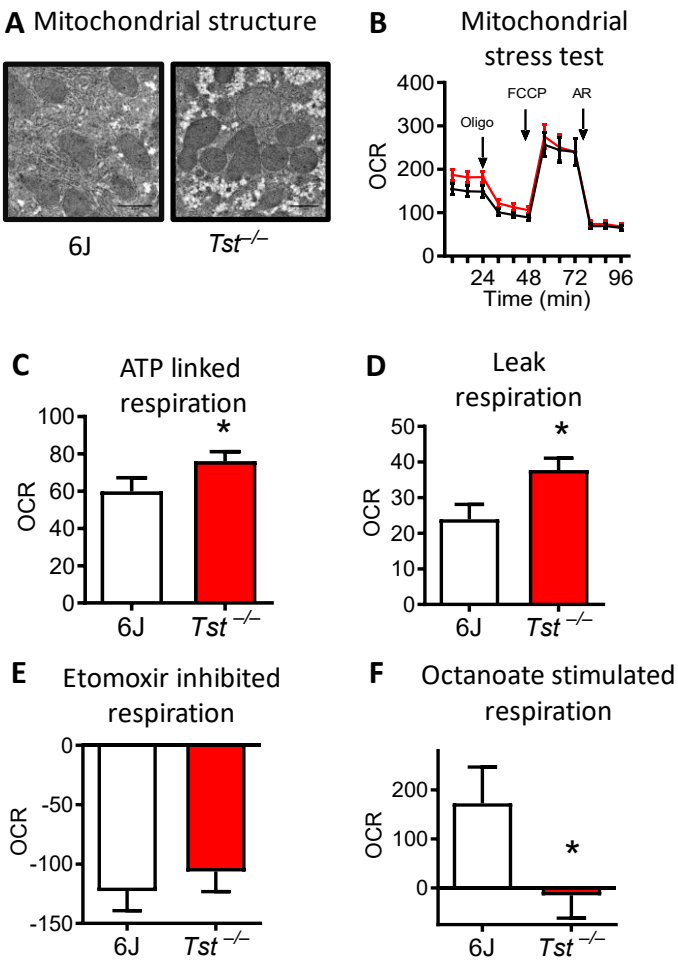

Figure 4. *Tst* deletion results in increased hepatocyte respiration but impaired medium–chain fat respiration. (**A**) Electron microscope images of liver, visualising mitochondria from normal diet-fed C57Bl/6J (n = 4) or *Tst*$^{-/-}$ (n = 4) mice. (**B**) Seahorse trace representing the mean oxygen consumption rate (OCR), normalised to protein, by hepatocytes from normal diet-fed C57Bl/6J (n = 6) or *Tst*$^{-/-}$ (n = 6) mice during a mitochondrial stress test. (**C**) Respiratory OCR linked to ATP production (oligomycin sensitive) by hepatocytes from normal diet-fed C57Bl/6J (n = 6) or *Tst*$^{-/-}$ (n = 6) mice, calculated from Figure 4B. (**D**) Respiratory OCR relating to proton leak (oligomycin insensitive) by hepatocytes from normal diet-fed C57Bl/6J (n = 6) or *Tst*$^{-/-}$ (n = 6) mice, calculated from Figure 4B. (**E**) Reduction of maximal uncoupled respiration following inhibition of long chain fatty acid mitochondrial import using etomoxir (8 µM), from normal diet-fed C57Bl/6J (n = 4) or *Tst*$^{-/-}$ (n = 4) mice. (**F**) Stimulation of maximal uncoupled respiration following addition of medium chain fatty acid octanoate (250 µM), from normal diet-fed C57Bl/6J (n = 4) or *Tst*$^{-/-}$ (n = 4) mice. Data are represented as mean ±SEM. Significance was calculated using an unpaired two tailed, student's t-test (**C**, **D**, **E**, **F**), * $P < 0.05$.

881 # Tables

Table 1. Sulfur species in blood, urine, tissue and cells				
	C57Bl/6J	***Tst*$^{-/-}$**	***Tst*$^{-/-}$/6J ratio**	**Significance**
A Trunk Blood (Micromolar)				
MBB-S (Sulfide)	2.28 +/- 0.43	22.18 +/- 0.85	9.73	****
MBB-SSO3 (Thiosulfate)	n.d.	6.25 +/- 3.17	n.c.	**ns**
B Trunk Plasma (Micromolar)				
MBB-S (Sulfide)	1.88 +/- 0.64	24.50 +/- 2.02	13.03	****
MBB-SSO3 (Thiosulfate)	3.99 +/- 0.99	80.29 +/- 13.6	20.12	**
MBB-GSH (reduced Glutathione)	48.0 +/- 1.15	86.25 +/- 6.27	1.80	***
C Urine (Micromoles/creatine/24hrs)				
MBB-SSO3 (Thiosulfate)	4.99 +/- 2.6	2374 +/- 319	475.75	****
D Inferior Vena Cava (Micromolar)				
MBB-S (Sulfide)	1.22 +/- 0.20	3.58 +/- 0.87	2.93	**ns (0.08)**
MBB-SSO3 (Thiosulfate)	6.58 +/- 4.51	88.3 +/- 13.0	13.42	*
E Liver (µmoles/kg wet liver)				
MBB-S (Sulfide)	13 +/- 1	17 +/- 3	1.31	**ns**
MBB-SSO3 (Thiosulfate)	4 +/- 1	15 +/- 7	3.75	**ns**
DNFB-GSH (reduced Glutathione)	6470 +/- 380	6850 +/- 30	1.04	**ns**
DNFB-Cysteine (Cysteine)	82 +/- 13	67 +/- 11	0.82	**ns**
F Sulfide P3 fluorescence (A510nm/protein)				
Hepatocyte	7.22 +/- 1.00	7.89 +/- 0.80	1.09	**ns**
G Mitochondrial sulfide (MitoA)				
Liver	0.78 +/- 0.16	1.14 +/- 0.45	1.46	**ns**
*** P < 0.05, ** P < 0.01, *** P < 0.001 **** P < 0.0001**				

882

883 **Table 1. *Tst* Deletion Results in Altered Sulfur Metabolites in Blood and Liver.** (**A**) Sulfide dibimane,
884 thiosulfate-MBB, measured by fluorescence detection following HPLC, from whole blood taken from
885 trunk blood of ND-fed C57Bl/6J (n = 4) and *Tst*$^{-/-}$ (n = 4) mice. (**B**) Sulfide dibimane, thiosulfate-MBB,
886 and rGSH-MBB, measured by fluorescence detection following HPLC, from EDTA-Plasma of ND-fed
887 C57Bl/6J (n = 4) and *Tst*$^{-/-}$ (n = 4) mice. (**C**) Thiosulfate-MBB corrected for creatinine from 24 hour
888 urine samples, taken from ND-fed C57Bl6/J (n = 4) and *Tst*$^{-/-}$ (n = 5) mice. (**D**) Sulfide dibimane, and
889 thiosulfate-MBB, from whole blood taken from the inferior vena cava downstream of the hepatic vein
890 of ND-fed C57Bl/6J (n = 3) and *Tst*$^{-/-}$ (n = 3) mice. (**E**) Sulfide dibimane, thiosulfate-MBB, rGSH-MBB,
891 and cysteine-MBB from whole liver (n=4/genotype) of ND-fed C57Bl/6J (n = 4) and *Tst*$^{-/-}$ (n = 4) mice.
892 (**F**) Fluorescence from cultured hepatocytes following incubation with P3 (sulfide reactive probe) from
893 ND-fed C57Bl/6J (n = 4) and *Tst*$^{-/-}$ (n = 4) mice. (**G**) Ratio of Mito N/MitoA from the liver of ND-fed
894 C57Bl/6J (n = 5) and *Tst*$^{-/-}$ (n = 5) mice. Data are represented as mean ±SEM. Significance was
895 calculated using unpaired two-tailed student's t-test. * P < 0.05, ** P < 0.01, *** P < 0.001, **** P <
896 0.0001
897

Table 2. GO Terms Persulfidation rate (*Tst*$^{-/-}$ vs C57Bl/6J liver, ND-fed)			
GO-ID	**Name**	**Direction (*Tst*$^{-/-}$ vs 6J)**	**Genes**
	GO terms Identified by log fold change		
0050660	FAD binding	Decreased	12
0008168	Methyltransferase activity	Decreased	9
0016741	Transferase activity, transferring one-carbon groups	Decreased	9
0008565	Protein transporter activity	Decreased	8
0008238	Exopeptidase activity	Decreased	7
0005777	Peroxisome	Decreased	7
0042579	Microbody	Decreased	7
0003995	Acyl-CoA dehydrogenase activity	Decreased	6
0008483	Transaminase activity	Decreased	6
0016769	Transferase activity, transferring nitrogenous groups	Decreased	6
0008757	S-adenosylmethionine-dependent methyltransferase activity	Decreased	6
0016655	Oxidoreductase activity, acting on NADH/NADPH, quinone	Decreased	5
0004177	Aminopeptidase activity	Decreased	5
0000059	Protein import into nucleus, docking	Decreased	3
0005643	Nuclear pore	Decreased	3
0031965	Nuclear membrane	Decreased	3
0044453	Nuclear membrane part	Decreased	3
0046930	Pore complex	Decreased	3
0015629	Actin cytoskeleton	Decreased	3
0016652	Oxidoreductase activity, NADH/NADPH, NAD/NADP acceptor	Decreased	3
0050662	Coenzyme binding	Increased	5
0016651	Oxidoreductase activity, NADH/NADPH,	Increased	5
0003954	NADH dehydrogenase activity	Increased	4
0008137	NADH dehydrogenase (ubiquinone) activity	Increased	4
0050136	NADH dehydrogenase (quinone) activity	Increased	4
0006739	NADP metabolism	Increased	3
0006769	Nicotinamide metabolism	Increased	3
0006733	Oxidoreduction coenzyme metabolism	Increased	3

898

899 **Table 2. Tst Deletion Results in Differential Persulfidation Rate of Liver Proteins**. Significant GO terms
900 represented by peptides with different persulfidation rates in the ND-fed *Tst*$^{-/-}$ liver relative to
901 C57Bl/6J. '**Direction**' indicates whether the persulfidation is decreased or increased in *Tst*$^{-/-}$ relative
902 to C57Bl/6J. '**Genes**' indicates the number of genes in the *Tst*$^{-/-}$ that represent the changes driving
903 the GO term.
904

905

906

907

908

Table 3. KEGG pathways (*Tst*$^{-/-}$ vs C57Bl/6J liver, ND-fed)			
Entry	**Name**	**Genes**	**Significance**
A. Increased in ND *Tst*$^{-/-}$ liver			
00250	Alanine, Aspartate and glutamate metabolism	6	***
00260	Glycine, serine and threonine metabolism	5	**
00270	Cysteine and methionine metabolism	4	*
04122	Sulfur relay system	2	*
B. Reduced in ND *Tst*$^{-/-}$ liver			
00980	Metabolism of xenobiotics by cytochrome P450	12	****
00982	Drug metabolism – cytochrome P450	12	****
05204	Chemical carcinogenesis	12	****
00480	Glutathione metabolism	8	***
00040	Pentose and glucoronate interconversions	5	**
04142	Lysosome	6	**
04390	Hippo signalling pathway	4	**
00500	Starch and sucrose metabolism	5	**
05215	Prostate cancer	3	**
04024	cAMP signalling pathway	4	*
04141	Protein processing in ER	9	*
05211	Renal cell carcinoma	3	*
00830	Retinol metabolism	6	*
00053	Ascorbate and aldarate metabolism	4	*
00860	Porphyrin and chlorophyll metabolism	4	*
04722	Neurotrophin signalling pathway	3	*
04670	Leukocyte transendothelial migration	4	*
04010	MAPK signalling pathway	4	*
04720	Long-term potentiation	2	*
04914	Progesterone-mediated oocyte maturation	2	*
04062	Chemokine signalling pathway	3	*
04110	Cell cycle	3	*
04015	Rap1 signaling pathway	4	*
00983	Drug metabolism - other enzymes	5	*
04918	Thyroid hormone synthesis	3	*
04612	Antigen processing and presentation	3	*
05203	Viral Carcinogenesis	5	*
*** P < 0.05, ** P < 0.01, *** P < 0.001 **** P < 0.0001**			

909

910 **Table 3. Tst Deletion Results in Differential Hepatic Protein Abundance of KEGG Pathways.** (**A**)
911 Significant KEGG pathway terms represented by proteins that are more abundant in the ND-fed *Tst*$^{-}$
912 $^{/-}$ liver compared with ND-fed C57Bl/6J. (**B**) Significant KEGG pathway terms represented by proteins
913 that are less abundant in the ND-fed *Tst*$^{-/-}$ liver compared with ND-fed C57Bl/6J. '**Genes**' indicates
914 the number of genes in the *Tst*$^{-/-}$ that represent the changes driving the KEGG pathway.

915

916

917

Table 4. GO Terms Congruence of Abundance and Persulfidation

GO-ID	Name	Persulfidation ($Tst^{-/-}$ vs 6J)	Abundance ($Tst^{-/-}$ vs 6J)
0008483	Transaminase activity	Decreased	Increased
0016769	Transferase activity, transferring nitrogenous	Decreased	Increased
0003995	Acyl-CoA dehydrogenase activity	Decreased	Decreased
0005777	Peroxisome	Decreased	Decreased
0042579	Microbody	Decreased	Decreased

918

919 **Table 4. The *Tst*$^{-/-}$ liver proteome and persulfidome converges on lipid oxidation pathways.** GO
920 terms that are significantly regulated following comparison of ND-fed *Tst*$^{-/-}$ relative to C57Bl/6J, at *both* the
921 level of cysteine persulfidation and protein abundance.

922

923